AGU PUBLICATIONS

Geophysical Research Letters

RESEARCH LETTER
10.1002/2017GL075703

Key Points:
- New measurements establish the low viscosity of a lunar magma ocean-relevant ferrobasalt at lunar *P-T* conditions (0.22–1.45 Pa s)
- Plagioclase would float on a low-viscosity lunar magma ocean to produce a crust with impure older units and very pure younger units
- Very pure crust in shallow impact basins and the lunar highlands is consistent with resurfacing of the Moon by lower crustal diapirs

Supporting Information:
- Supporting Information S1

Correspondence to:
N. Dygert,
ndygert1@utk.edu

Citation:
Dygert, N., Lin, J.-F., Marshall, E. W., Kono, Y., & Gardner, J. E. (2017). A low viscosity lunar magma ocean forms a stratified anorthitic flotation crust with mafic poor and rich units. *Geophysical Research Letters*, *44*. https://doi.org/10.1002/2017GL075703

Received 15 SEP 2017
Accepted 27 OCT 2017
Accepted article online 31 OCT 2017

A Low Viscosity Lunar Magma Ocean Forms a Stratified Anorthitic Flotation Crust With Mafic Poor and Rich Units

Nick Dygert[1,2], Jung-Fu Lin[1], Edward W. Marshall[1], Yoshio Kono[3], and James E. Gardner[1]

[1]Department of Geological Sciences, Jackson School of Geosciences, University of Texas at Austin, Austin, TX, USA, [2]Planetary Geosciences Institute, Department of Earth and Planetary Sciences, University of Tennessee, Knoxville, Knoxville, TN, USA, [3]HPCAT, Geophysical Laboratory, Carnegie Institution of Washington, Argonne, IL, USA

Abstract Much of the lunar crust is monomineralic, comprising >98% plagioclase. The prevailing model argues the crust accumulated as plagioclase floated to the surface of a solidifying lunar magma ocean (LMO). Whether >98% pure anorthosites can form in a flotation scenario is debated. An important determinant of the efficiency of plagioclase fractionation is the viscosity of the LMO liquid, which was unconstrained. Here we present results from new experiments conducted on a late LMO-relevant ferrobasaltic melt. The liquid has an exceptionally low viscosity of $0.22^{+0.11}_{-0.19}$ to $1.45^{+0.46}_{-0.82}$ Pa s at experimental conditions (1,300–1,600°C; 0.1–4.4 GPa) and can be modeled by an Arrhenius relation. Extrapolating to LMO-relevant temperatures, our analysis suggests a low viscosity LMO would form a stratified flotation crust, with the oldest units containing a mafic component and with very pure younger units. Old, impure crust may have been buried by lower crustal diapirs of pure anorthosite in a serial magmatism scenario.

Plain Language Summary This manuscript reports the first experimental measurements of the viscosity of a late lunar magma ocean liquid. Sample studies and remote sensing suggest the Moon's crust is effectively composed of one mineral (plagioclase). The crust is thought to have formed by flotation of buoyant plagioclase on a crystallizing lunar magma ocean; whether such a pure crust can form in a flotation scenario is debated. The purity of a flotation crust crucially depends on the viscosity of the magma ocean which was previously unconstrained. Experiments were conducted at high pressure-temperature conditions at Argonne National Laboratory to characterize viscosity. Measured viscosities are as low as or lower than geologically-relevant silicate melts measured previously. In a two part analysis, we consider the effect of the low viscosity lunar magma ocean on the purity of the crust. We conclude that the oldest flotation crust will contain a significant mafic component, while younger portions of the flotation crust will be pure, resulting in a stratified crust with mafic poor and rich units. The high purity of the present-day lunar crust surface can best be explained by ancient resurfacing of the crust by the rise of buoyant lower crustal diapirs.

1. Introduction

The lunar crust is dominantly composed of remarkably pure anorthosite. Near-infrared spectroscopy suggests that in the highlands region and in many impact basins it is >98% pure (Donaldson-Hanna et al., 2014; Ohtake et al., 2009), containing only trace amounts of mafic phases (pyroxenes and olivine). Sample studies paint a consistent picture, with "pristine" samples comprising up to 99.5% pure anorthite (Warren, 1990, and references therein). The formation of such pure igneous rocks on any planetary body is rare and has fueled ongoing debate about the origin of the crust. The prevailing view is that buoyant plagioclase floated on the crystallizing lunar magma ocean (LMO) after the Moon-forming giant impact, accumulating to form an anorthositic crust (e.g., Walker & Hays, 1977, Wood et al., 1970). Others argue it was emplaced as diapirs in a serial magmatism process after lunar magma ocean crystallization (e.g., Jolliff & Haskin, 1995; Longhi, 2003; Walker, 1983), or by mineral segregation from magma chambers akin to those that may have formed terrestrial anorthosites, with or without a magma ocean (Longhi & Ashwal, 1985; Morse, 1982). Because the efficiency of crystal fractionation depends significantly on the viscosity of the magma ocean liquid, constraints on viscosity are critical for evaluating whether a pure flotation crust can form. For example, melt viscosity affects the convective vigor and turbulence of magma oceans (e.g., Abe, 1997; Solomatov, 2007), rates of Stokes' settling and/or flotation, length scales of hydrodynamic interactions among suspended particles (e.g., Koyaguchi et al., 1990; Suckale et al., 2012), and viscous drag forces that

entrain and maintain crystals in suspension in convecting liquids (e.g., Solomatov et al., 1993). Additionally, melt viscosity plays a critical role in determining rates of melt percolation through a crystalline matrix and the characteristic compaction length of a cumulate pile (e.g., McKenzie, 1984). Estimates for LMO viscosities differ by as much as 2 orders of magnitude (1–100 Pa s, Piskorz & Stevenson, 2014; Suckale et al., 2012). Here we present new experimental measurements that constrain viscosity of the plagioclase-saturated LMO. We use our experimental results to analyze the efficiency of plagioclase fractionation throughout LMO solidification and compaction of trapped liquid out of the crust. We predict the formation of a stratified anorthositic flotation crust composed of mafic poor and rich units.

2. Experiments

Falling sphere viscometry experiments were conducted at Beamline 16-BMB at the Advanced Photon Source, Argonne National Laboratory, using a Paris-Edinburgh large volume press (Kono, Park, et al., 2014). A brief description of the experimental methods follows; full details are given in the supporting information. A rhenium sphere is placed at the top of a graphite-lined BN capsule packed with oxide powders. The experiment is heated to its estimated solidus temperature and then flash melted, causing the sphere to sink and accelerate to its terminal velocity. The trajectory of the falling sphere is recorded by a high-speed camera (in this case, at 50 frames/s). Kono et al. (2015) discussed requirement of high-speed imaging to measure high falling sphere velocity in low viscosity melts. Our measured falling velocity is 0.1 to 0.5 mm/s; a 50 fps camera frame rate monitors more than 200 frames in the falling sphere trajectory, which are sufficient to accurately determine the viscosity of the melts. The viscosity of the liquid is calculated using Stokes' law with wall and end effect corrections. Because the Paris-Edinburgh apparatus lacks a thermocouple, the target temperature is attained using an experimentally calibrated current *T* curve (Kono, Park, et al., 2014); based on well-known melting temperatures of salts we estimate the uncertainty to be ±5% (e.g., Kono et al., 2013; Kono, Kenney-Benson, et al., 2014). Pressure is calculated from direct energy dispersive X-ray diffraction measurement of MgO in an assembly component using an equation of state of MgO (Kono et al., 2010), accurate to ~ ± 0.2 GPa.

The starting material is an Fe- and Ti-rich ferrobasalt prepared from reagent grade oxide powders, representing a plagioclase saturated residual magma ocean liquid after 95% crystallization of the LMO (Longhi, 2003). This melt is an important compositional end-member for the plagioclase saturated LMO; its viscosity has not been measured previously. To characterize the composition of the mixture, experimental powders were fused in a piston cylinder run. Electron microprobe analysis determined the following composition (in wt %): SiO_2, 43.7; TiO_2, 3.8; Al_2O_3, 9.5; CaO, 11.8; FeO, 28.2; MgO, 0.3; MnO, 0.6; Na_2O, 0.7; K_2O, 0.22, in good agreement with the target composition (FR-1290, Dygert et al., 2013, 2014; Longhi, 2003). Fourier transform infrared spectroscopic analysis of an experimental run product yielded an H_2O_T content of 0.44 ± 0.01 wt % assuming an absorption coefficient of 63 L/mol (e.g., Mandeville et al., 2002). Presumably, this originates from water adsorbed on starting powders and assembly components as no water was added to the starting material. A water content of 0.44 wt % is consistent with that expected after 95% crystallization of a lunar magma ocean with the estimated bulk water content of the Moon (100–300 ppm, Hauri et al., 2015), which would be on the order of 0.2–0.6 wt %.

3. Results and Analysis

Experimental results are summarized in Table 1 and Figure 1. The measurements demonstrate the viscosity of the liquid is pressure insensitive under the conditions explored (1,300–1,600°C, 0.1–4.4 GPa, Figure 1a) and can be modeled by an Arrhenius relation with an activation energy of 153 ± 30 kJ/mol and preexponential of $1.10\times10^{-5}{}^{+7.26\times10^{-5}}_{-8.89\times10^{-6}}$ (Figure 1b). At experimental conditions, the liquid has a viscosity as low as or lower than many geologically relevant silicate liquids investigated previously ($0.25^{+0.06}_{-0.04}$ to $1.45^{+0.58}_{-0.38}$ Pa s; comparison with the compilation of Hui and Zhang, 2007 is shown in Figure 1c). Figure 1d compares our viscosity results with liquids of a variety of compositions, allowing some qualitative inferences about the influence of melt structure on viscosity to be made. Andesite has similar temperature sensitivity but viscosities an order of magnitude higher than our liquid, presumably owing to its higher silica content and greater degree of polymerization. Carbonate melt is much less viscous, owing to its lack of network-forming Si tetrahedra. Our melt is similar to liquid peridotite, both being relatively silica poor. Our melt, however, contains significantly more molar Na, Ca, and Ti relative to molar Si. Na, Ca, and Ti are network modifying cations that

Table 1
Summary of Experimental Results

Experiment	T (°C)[a]	P (Gpa)[a]	η (Pa s)
2	1,400	0.1	$0.49^{+0.22}_{-0.38}$
3	1,400	3.3	$0.86^{+0.22}_{-0.38}$
4	1,400	4.1	$0.62^{+0.22}_{-0.38}$
5	1,300	2.2	$1.45^{+0.46}_{-0.82}$
7	1,500	4.4	$0.23^{+0.11}_{-0.19}$
9	1,500	2.2	$0.44^{+0.11}_{-0.19}$
11	1,400	2	$0.51^{+0.22}_{-0.38}$
12	1,500	2.9	$0.22^{+0.11}_{-0.19}$
14	1,600	1.5	$0.25^{+0.06}_{-0.10}$
16	1,500	1.5	$0.38^{+0.11}_{-0.19}$

[a]Nominal. Estimated uncertainties are ±5% for temperature and 0.2 GPa for pressure.

form nonbridging bonds with silicon tetrahedra (Hess, 1995), disrupting longer-range structures that might form otherwise, possibly explaining the lower viscosity of our ferrobasalt compared to peridotite.

Recent models for predicting the viscosity of silicate liquids as a function of composition and temperature successfully reproduce experimental viscosity determinations for a wide array of compositional systems (Giordano et al., 2008; Hui & Zhang, 2007; Sehlke & Whittington, 2016). We evaluated the ability of these predictive models to reproduce our experimental observations (supporting information Figure S2). All the models appear to accurately reproduce the temperature dependence of our melt viscosity. Hui and Zhang (2007) predict the measured viscosities within experimental uncertainty, but the models of Giordano et al. (2008) and Sehlke and Whittington (2016) overestimate the measured viscosities by roughly

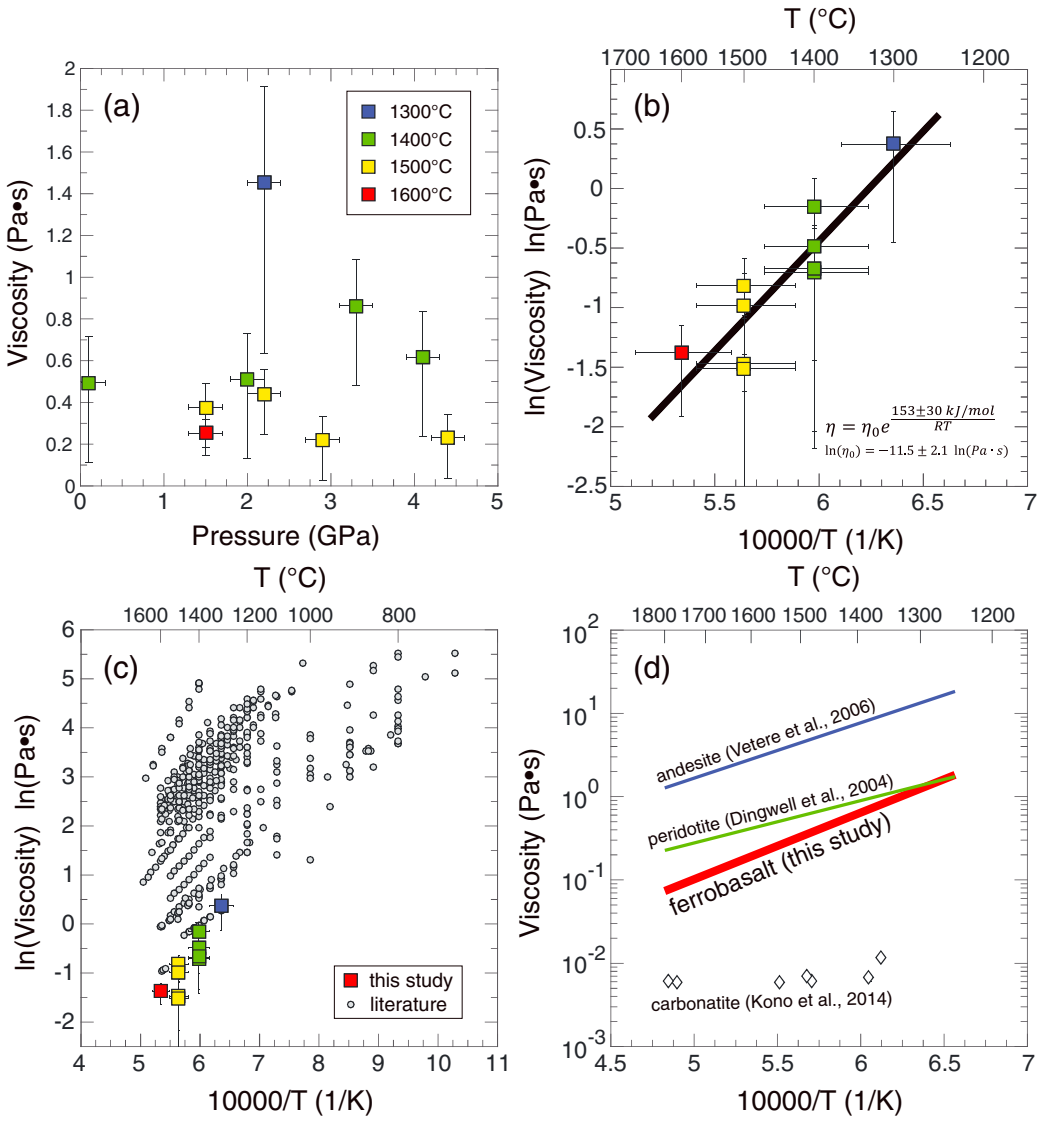

Figure 1. Summary of the experimental results. (a) Viscosity plotted as a function of pressure. No systematics are observed. (b) Log viscosity plotted against inverse temperature. (c) Comparison among the new experimental results and superliquidus experiments on silicate melts from the literature (compilation of Hui and Zhang 2007). (d) Comparison of viscosity predicted by our Arrhenius relation to geologic materials as a function of temperature.

a factor of 2. The overestimation may be attributed to the model calibrations and/or compositional extrapolation from the calibration data sets.

4. The Evolving Viscosity and Density of the LMO

Because Stokes' settling rates, particle entrainment in convecting magma ocean liquids, and interactions among suspended particles depend on the viscosity of the magma ocean liquid (e.g., Elkins-Tanton, 2012; Solomatov et al., 1993; Suckale et al., 2012), the purity of the ferroan anorthositic crust largely depends on the viscosity of the LMO, which evolved throughout plagioclase crystallization. Our Arrhenius relation places an important bound on the viscosity of the LMO at end-stage (~95%) solidification. However, the LMO first became plagioclase saturated when it was ~80% solidified and had a relatively less evolved (more magnesian, less Ti, Ca, and Na rich) composition (e.g., Longhi, 2003). We must estimate the viscosity and density of the LMO throughout the duration of plagioclase crystallization to evaluate how magma ocean dynamics affected the purity of the entire anorthositic flotation crust.

LMO liquid viscosity and density can be estimated using composition and temperature output from MAGFOX (Longhi, 1991), an experimentally calibrated fractional crystallization program developed to predict LMO liquid and cumulate compositions throughout LMO solidification for an assumed LMO bulk composition. Fractional crystallization experiments evaluating LMO cumulate and liquid compositions as a function of the degree of LMO solidification were also recently published (Lin et al., 2017a, 2017b). Liquid compositions from plagioclase saturated experiments and two MAGFOX models (run assuming two different LMO bulk compositions) were input into predictive viscosity models to estimate reasonable bounds on LMO viscosity (dry and with 0.5 wt % H_2O) and are presented in Figure 2a as a function of Mg# (100×Mg/Mg+Fe, in moles) and Figure 2b as a function of temperature.

Regardless of model, the relative LMO viscosity is predicted to increase as LMO solidification proceeds owing to the balance between competing effects of cooling and compositional evolution (i.e., progressive enrichment of network modifying cations in the LMO liquid as Mg# decreases). However, absolute values for viscosity differ significantly among models, particularly at end-stage LMO solidification, where values as high as ~70 Pa s are predicted. Our Arrhenius relation based on direct experimental viscosity measurements of a melt relevant to the late LMO places a more robust constraint on late LMO viscosity than predictive models, which are all extrapolated from their calibration data sets. Assuming an atmospheric pressure liquidus temperature of 1,000°C for our melt (Longhi, 2003), we estimate a LMO viscosity of ~20 Pa s at end-stage solidification. We note this is in good agreement with predictions of Hui and Zhang, 2007 for both the experimentally produced LMO liquids and the MAGFOX models. Thus, we argue the plagioclase saturated LMO evolved from a viscosity of ~1 Pa s at the onset of plagioclase crystallization (when T and Mg# were relatively high) to ~20 Pa s at end-stage crystallization (when T and Mg# were relatively low). These improved viscosity estimates refine calculation of crystal sinking/floating rates in the plagioclase-saturated LMO (supporting information Figure S3), and constrain conditions under which crystal suspension in convecting LMO liquids is possible (section 5).

Knowledge of the LMO liquid composition throughout plagioclase crystallization enables us to calculate the density of the LMO liquid, which is important for estimating fractionation efficiency. Based on calculations made using an atmospheric pressure partial molar volume method (Dixon et al., 1995; Lange & Carmichael, 1990), we estimate the LMO liquid density increased from ~2,900 kg/m^3 at plagioclase saturation to 3,300 kg/m^3 at end-stage solidification owing to progressive enrichment of Fe and Ca in the melt as crystallization proceeded (Figure 2c). The density of the liquid would have been ~5% higher at the base of the LMO (Vander Kaaden et al., 2015); the maximum possible depth of the plagioclase saturated LMO (assuming an initially whole Moon magma ocean) is ~120 km, corresponding to a pressure of ~0.6 GPa. Our results suggest that plagioclase ($\rho < 2{,}800$ kg/m^3) was sufficiently buoyant throughout LMO solidification to raft denser mafic minerals into the flotation crust (Warren, 1990).

5. Purity of an Anorthositic Flotation Crust

Plagioclase crystallization occurred in downwelling plumes that originated from a thermal boundary layer near the magma ocean surface (Parmentier et al., 2007) and at the base of the LMO where the adiabat crossed the liquidus (Walker et al., 1975). Formation of a pure anorthositic flotation crust requires that buoyant

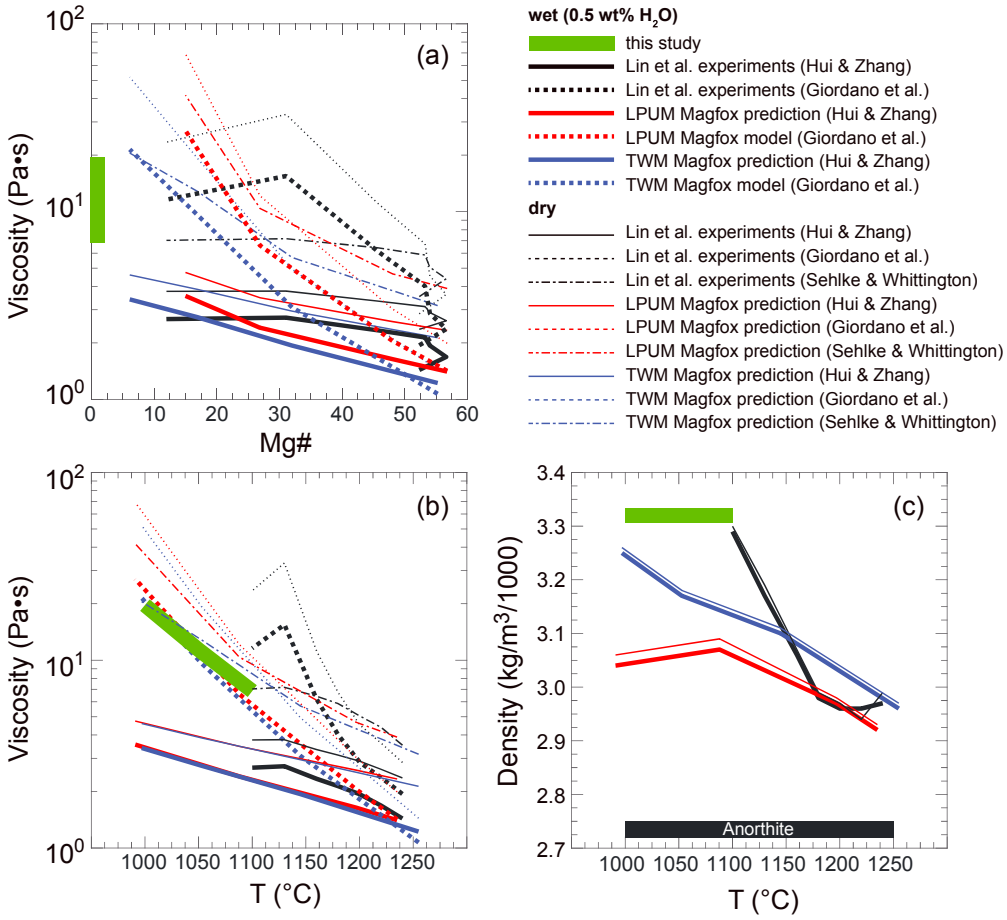

Figure 2. (a and b) Viscosities predicted by our Arrhenius relation (thick green line) compared to predictions of the models of Hui and Zhang 2007, Giordano et al. 2008, and Sehlke and Whittington 2016 for three possible plagioclase saturated lunar magma oceans and (c) atmospheric pressure densities of the LMO liquids. Shown in Figure 2a is the evolution of viscosity with Mg#; shown in Figure 2b is the evolution of viscosity with temperature. Mg# and *T* decreased as the LMO crystallized. Black lines are predictions for experiments of Lin et al. (2017a); red lines show MAGFOX predictions (e.g., Longhi, 1991) for a magma ocean with an Earth-like Lunar Primitive Upper Mantle (LPUM) bulk composition (Hart & Zindler, 1986); and blue lines show MAGFOX predictions for a more plagioclase normative Taylor Whole Moon (TWM) bulk composition (Taylor, 1982). Thick lines are for melts with 0.5 wt % H_2O; thin lines are for dry melts. MAGFOX is a fractional crystallization program developed by John Longhi, specifically calibrated for lunar magma ocean compositions and *P-T* conditions.

plagioclase crystals rose to the surface of the LMO, and that dense mafic cumulates (olivine and pyroxenes) sank to become part of the cumulate pile rather than being rafted into the crust (Figure 3b). Velocities for Stokes' flow of buoyant plagioclase crystals are rapid compared to time scales of LMO solidification (supporting information Figure S3). However, convection in the LMO would have affected the efficiency of flotation (i.e., crystal fractionation). For example, authors have argued for batch rather than fractional crystallization during the first 50% of LMO solidification owing to early vigorous convection (e.g., Synder et al., 1992). Crystal entrainment in LMO convection cells would mix low and high density phases, producing an impure flotation crust (Figure 3a). Solomatov et al. (1993) derived an expression that predicts particle entrainment in convecting liquids applicable to both laminar and turbulent convection

$$D = \frac{1}{\Delta\rho g}\left(\frac{0.1\eta\alpha F}{C_P}\right)^{\frac{1}{2}} \quad (1)$$

where D is the critical grain diameter for entrainment, $\Delta\rho$ is the density difference between particles and liquid, g is the gravitational acceleration, η is the viscosity of the liquid, α is the coefficient of thermal expansion (for the LMO, ~3×10^{-5}/K), C_P is heat capacity (~800 J/kg/K), and F is the heat flux.

Before the onset of plagioclase crystallization, assuming no primitive atmosphere or quench crust, the LMO would have experienced vigorous convection beneath a free surface with a heat flux on the order of

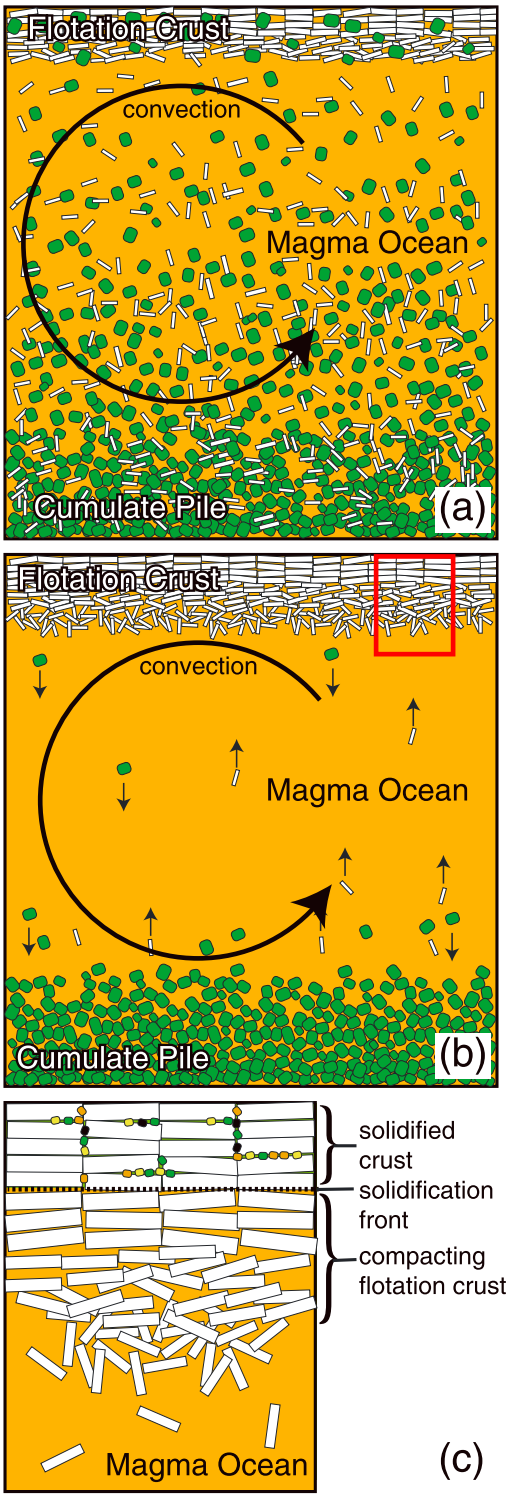

Figure 3. Cartoons illustrating end-member scenarios for solidification of the LMO after plagioclase saturation. Green minerals represent mafics, and white minerals represent plagioclase. (a) Case where crystals are efficiently entrained and maintained in suspension, forming agglomerations of phases that put dense mafics into the flotation crust and buoyant plagioclase into the cumulate pile. (b) Case where crystals are not entrained in the convecting magma ocean resulting in efficient fractionation of low and high density phases. Red square indicates area shown in Figure 3c. (c) Schematic showing the propagation of a solidification front into an accumulating and compacting flotation crust. Melt not squeezed out of the flotation crust precipitates mafic minerals and ilmenite.

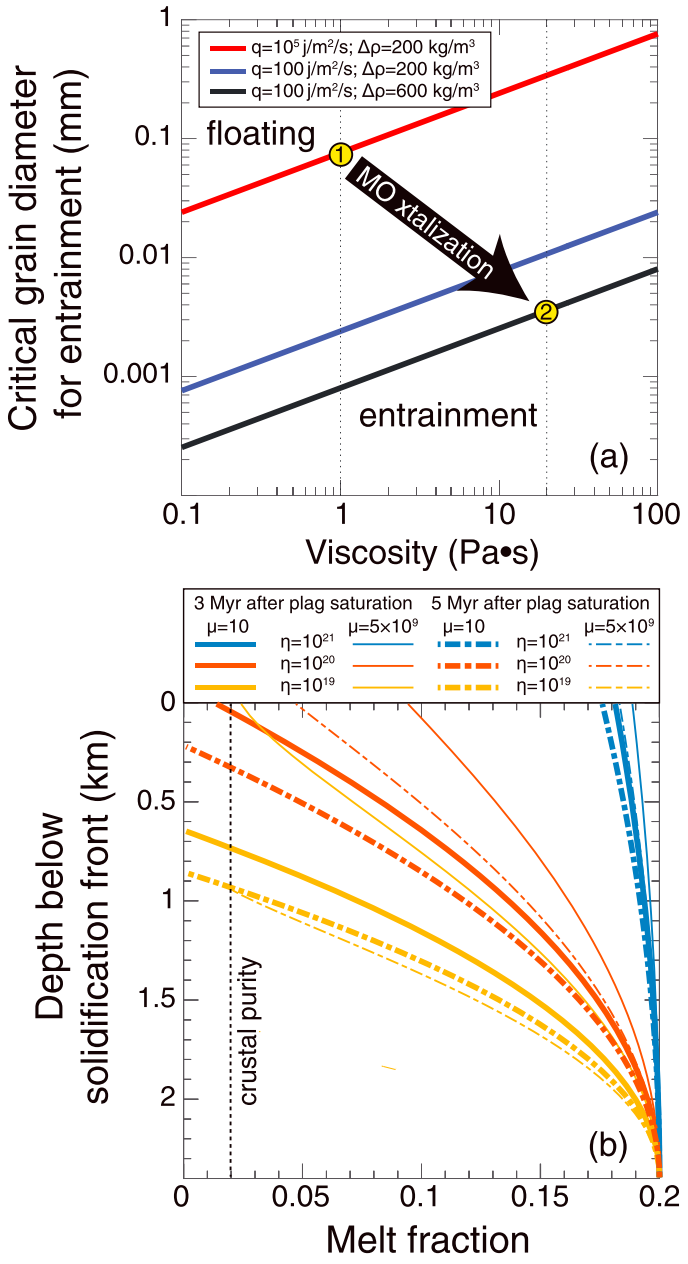

Figure 4. (a) Critical grain sizes for entrainment predicted by equation (1) as a function of melt viscosity. As indicated by the black arrow, properties of the magma ocean evolve from (1) to (2) as crystallization proceeds. (b) Solutions to the model of Piskorz and Stevenson (2014) for different assumptions of melt viscosity (μ) and compaction viscosity (η) at 2 times after initial formation of a flotation crust. The vertical axis shows depth in the crust beneath the solidification front (see Figure 3c), and the horizontal axis shows the melt fraction. Solutions are presented for two assumptions of melt viscosity, 10 Pa s (thick lines) and 5×10^9 Pa s (thin lines), and the latter was chosen as it is just above the viscosity needed to produce deviations from low viscosity solutions. Solutions after 3 Myr of flotation crust formation are shown as solid lines, those after 5 Myr crust formation are shown as dashed lines. Colors indicate the assumed compaction viscosity. The model is not sensitive to melt viscosity within LMO-relevant bounds; cases that produce melt fractions consistent with the observed crustal purity have compaction viscosities $\lesssim 10^{20}$ Pa s. The density difference between plagioclase and melt was assumed to be 200 kg/m^3, and other parameters are assumed by Piskorz and Stevenson (2014).

10^5 J/m^2 (e.g., Elkins-Tanton et al., 2011). The eventual accumulation of a flotation crust would impose conductive heat loss, reducing heat flux by many orders of magnitude (e.g., a conductively cooling 100 m thick flotation crust would permit a heat flux of ~100 J/m^2). Critical grain diameters predicted by equation (1) are shown in Figure 4a as a function of viscosity for two choices of heat flux. At the onset of plagioclase saturation, heat flux was high but the viscosity of the LMO was low; plagioclase grains larger than 0.1 mm would have floated while smaller grains remained entrained in the convecting LMO. As crystallization proceeded and a flotation crust began to form, heat flux decreased dramatically while the viscosity and density of the LMO increased. Periodic disruption of the flotation crust by impact bombardment would temporarily increase cooling rates by creating fracture networks and "thermal holes" in the forming flotation crust (e.g., Perera et al., 2017). Impact bombardment would also mechanically mix flotation crust, LMO liquid, and impactor, and introduce a secondary heat source. These events would sporadically increase the critical grain size for entrainment while the crust was still thin (heat flux from a convecting blackbody scales as T^4 while the heat flux through a conductively cooling crust scales with the temperature gradient across the crust). During end-stage LMO solidification, when the flotation crust was relatively thick and conductively cooling, the critical grain diameter for entrainment was $<$100 μm. We note that an alternative analysis of particle entrainment in the convecting LMO based on energy balance recovers consistent grain size estimates (supporting information Figure S4).

Because the growth of plagioclase crystals strongly depends on cooling rate (e.g., Walker et al., 1978; supporting information Figure S5), rapid cooling at the onset of plagioclase crystallization would have produced plagioclase crystals small enough to be entrained in convection cells along with mafic phases. Suckale et al. (2012) numerically investigated interactions among buoyant and negatively buoyant crystals in convecting liquids and found that agglomerations of crystals form when the suspended crystal fraction is ~10%. The early lunar flotation crust may have been composed of clumps of low density plagioclase laths and rafted denser mafic phases (e.g., Figure 3a). As the accumulating crust slowed down cooling of the LMO, cumulate plagioclase and mafic phases would have grown larger than the critical grain size for entrainment and rapidly sank or floated as Stokes' solids, forming a relatively pure anorthitic flotation crust with some interstitial magma ocean melt (Figure 3c and supporting information Figures S3 and S5). In addition to forming a relatively pure flotation crust, efficient crystal fractionation would have minimized the amount of low density plagioclase in the mafic cumulate pile, maximizing the driving force for lunar cumulate mantle overturn (e.g., Dygert et al., 2016; Hess & Parmentier, 1995; Ringwood & Kesson, 1976).

Melt-bearing crust would experience gravitational compaction, squeezing interstitial melt back into the LMO. As the melt-bearing crust cooled, mafic minerals would have precipitated from any trapped liquids present behind a solidification front that propagated downward into the accumulating crust (Figure 3c). To form a pure flotation crust, the rate of compaction or squeezing of trapped liquid out

of the accumulating crust must exceed the propagation rate of the solidification front. Piskorz and Stevenson (2014) developed a compaction-solidification model to estimate the amount of trapped liquid frozen into the flotation crust. Assuming conductive cooling, they argue the solidification front propagates downward at a rate proportional to the square root of inverse time, and that melt escapes the crust by Darcy flow facilitated by compaction. In their analysis, they assumed a melt viscosity 1–2 orders of magnitude greater than our experimental and model-based estimates. We tested the sensitivity of their result to melt viscosity and found compaction is impeded at melt viscosities much greater than the experimental constraints (compare thin and thick lines, Figure 4b). For reasonable melt viscosities and any choice of compaction viscosity, crust produced early contains more trapped melt than crust produced a few Myr later (compare thick solid and dashed lines, Figure 4b), because the solidification front propagates downward more slowly as the crust thickens.

6. Implications

Our analysis suggests that the oldest part of the flotation crust had a mafic fraction $>>$ 2% owing to rafting of mafic phases in the low viscosity LMO liquid when heat flux was high. Rafting may have continued after some crustal accumulation if impact bombardment significantly increased the heat flux across the juvenile crust. Solidification of trapped low viscosity liquids in the accumulating crust would contribute to the crustal mafic fraction while compaction of LMO liquid out of the crust was ineffective. Formation of a high-purity flotation crust is expected after ~5 Myr of LMO solidification, assuming compaction viscosities of ~10^{20} Pa s or less. Exposure of $>$98% pure anorthosites on the lunar surface requires that the oldest units in the flotation crust were removed by impact erosion (e.g., Piskorz & Stevenson, 2014), or that they were displaced and buried by more pure, hot lower crustal diapirs in a serial magmatism process (e.g., Jolliff & Haskin, 1995; Longhi, 2003; Walker, 1983). The latter can be thought of as effective "crustal overturn."

We envision a present-day lunar flotation crust composed of a layer of relatively impure, older crust intruded by a multitude of pure younger diapirs by serial magmatism. This mechanism can reconcile the observation of adjacent bodies of mafic-poor and mafic-rich lower crust in impact rings, basins, and central peaks (Baker & Head, 2015; Cahill et al., 2009; Cheek et al., 2013; Donaldson Hanna et al., 2014). Longhi (2003) proposed that the heat source driving serial magmatism is cumulate mantle overturn, which would have juxtaposed hot, early LMO cumulates from the deep lunar interior against the base of the flotation crust within a few hundred million years of lunar formation (e.g., Hess & Parmentier, 1995). Overturn is also thought to have produced the Mg-suite volcanism that intruded the lunar crust (e.g., Hess, 2006). Introduction of heat by cumulate mantle overturn could partially or completely reset isotopic ages of crustal bodies, explaining observation of relatively young ages of some ferroan anorthosites (e.g., 4.360 ± 3 Gyr, Borg et al., 2011), and overlap or near overlap among ferroan anorthosite and Mg-suite ages (e.g., 4.45 ± 0.27 to 4.283 ± 0.023 Gyr, Carlson et al., 2014).

According to the LMO crystallization experiments and our MAGFOX models, the Mg# of the mafic component in impure crustal units should be $\lesssim$80 (e.g., Lin et al., 2017b), in agreement with pristine Apollo samples (Papike et al., 1998). Our analysis suggests that the most important remaining uncertainties in predicting the mafic fraction in a lunar flotation crust are the evolution of the LMO heat flux (Figure 4a) and the crustal compaction viscosity (Figure 4b). Future work could attempt to estimate compaction viscosity, heat flux, and the LMO solidification time scale using observed variations in mafic fraction.

Acknowledgments

We thank Kerri Donaldson Hanna and an anonymous reviewer for comments that significantly improved this manuscript. This work was supported by a postdoctoral fellowship to N. D. by the Jackson School of Geosciences. The experiments were performed at HPCAT (Sector 16), Advanced Photon Source (APS), Argonne National Laboratory. HPCAT operation is supported by DOE-NNSA under award DE-NA0001974, with partial instrumentation funding by NSF. The Advanced Photon Source is a U.S. Department of Energy (DOE) Office of Science User Facility operated for the DOE Office of Science by Argonne National Laboratory under contract DE-AC02-06CH11357. J. F. L acknowledges support from NSF Geophysics Program and Extreme Physics and Chemistry Program of the Deep Carbon Observatory. Y. K. acknowledges the support of DOE-BES/DMSE under award DE-FG02-99ER45775 and support by the National Science Foundation under award EAR-1722495. J. E. G. acknowledges support by the National Science Foundation under award OCE-1333882. Raw experimental data are available on request to N. D.

References

Abe, Y. (1997). Thermal and chemical evolution of the terrestrial magma ocean. *Physics of the Earth and Planetary Interiors*, *100*(1-4), 27–39. https://doi.org/10.1016/S0031-9201(96)03229-3

Baker, D. M. H., & Head, J. W. (2015). Constraints on the depths of origin or peak rings on the Moon from Moon Mineralogy Mapper data. *Icarus*, *258*, 164–180. https://doi.org/10.1016/j.icarus.2015.06.013

Borg, L. E., Connelly, J. N., Boyet, M., & Carlson, R. W. (2011). Chronological evidence that the Moon is either young or did not have a global magma ocean. *Nature*, *477*(7362), 70–72. https://doi.org/10.1038/nature10328

Cahill, J. T. S., Lucey, P. G., & Wieczorek, M. A. (2009). Compositional variations of the lunar crust: Results from radiative transfer modeling of central peak spectra. *Journal of Geophysical Research*, *114*, E09001. https://doi.org/10.1029/2008JE003282

Carlson, R. W., Borg, L. E., Gaffney, A. M., & Boyet, M. (2014). Rb-Sr, Sm-Nd and Lu-Hf isotope systematics of the lunar Mg-suite: The age of the lunar crust and its relation to the time of Moon formation. *Philosophical Transactions of the Royal Society A*, *372*. https://doi.org/10.1098/rsta.2013.0246

Cheek, L. C., Donaldson Hanna, K. L., Pieters, C. M., Head, J. W., & Whitten, J. L. (2013). The distribution and purity of anorthosite across the Orientale basin: New perspectives from Moon Mineralogy Mapper data. *Journal of Geophysical Research: Planets*, *118*, 1805–1820. https://doi.org/10.1002/jgre.20126

Dingwell, D. B., Courtial, P., Giordano, D., & Nichols, A. R. L. (2004). Viscosity of peridotite liquid. *Earth and Planetary Science Letters*, *226*(1-2), 127–138. https://doi.org/10.1016/j.epsl.2004.07.017

Dixon, J. E., Stolper, E. M., & Holloway, J. R. (1995). An experimental study of water and carbon dioxide solubilities in mid-ocean ridge basaltic liquids. Part I: Calibration and solubility of melts. *Journal of Petroleum*, *36*(6), 1607–1631.

Donaldson Hanna, K. L., Cheek, L. C., Pieters, C. M., Mustard, J. F., Greenhagen, B. T., Thomas, I. R., & Bowles, N. E. (2014). Global assessment of pure crystalline plagioclase across the Moon and implications for the evolution of the primary crust. *Journal of Geophysical Research: Planets*, *119*, 1516–1545. https://doi.org/10.1002/2013JE004476

Dygert, N., Hirth, G., & Liang, Y. (2016). A flow law for ilmenite in dislocation creep: Implications for lunar cumulate mantle overturn. *Geophysical Research Letters*, *43*, 532–540. https://doi.org/10.1002/2015GL066546

Dygert, N., Liang, Y., & Hess, P. (2013). The importance of melt TiO_2 in affecting major and trace element partitioning between Fe-Ti oxides and lunar picritic glass melts. *Geochimica et Cosmochimica Acta*, *106*, 134–151. https://doi.org/10.1016/j.gca.2012.12.005

Dygert, N., Liang, Y., Sun, C., & Hess, P. (2014). An experimental study of trace element partitioning between augite and Fe-rich basalts. *Geochimica et Cosmochimica Acta*, *132*, 170–186. https://doi.org/10.1016/j.gca.2014.01.042

Elkins-Tanton, L. T. (2012). Magma oceans in the inner solar system. *Annual Review of Earth and Planetary Sciences*, *40*(1), 113–139. https://doi.org/10.1146/annurev-earth-042711-105503

Elkins-Tanton, L. T., Burgess, S., & Yin, Q.-Z. (2011). The lunar magma ocean: Reconciling the solidification process with lunar petrology and geochemistry. *Earth and Planetary Science Letters*, *304*(3-4), 326–336. https://doi.org/10.1016/j.epsl.2011.02.004

Giordano, D., Russell, J. K., & Dingwell, D. B. (2008). Viscosity of magmatic liquids: A model. *Earth and Planetary Science Letters*, *271*(1-4), 123–134. https://doi.org/10.1016/j.epsl.2008.03.038

Hart, S. R., & Zindler, A. (1986). In search of a bulk-Earth composition. *Chemical Geology*, *57*(3-4), 247–267. https://doi.org/10.1016/0009-2541(86)90053-7

Hauri, E. H., Saal, A. E., Rutherford, M. J., & Van Orman, J. A. (2015). Water in the Moon's interior: Truth and consequences. *Earth and Planetary Science Letters*, *409*, 252–264. https://doi.org/10.1016/j.epsl.2014.10.053

Hess, P. C. (1995). Thermodynamic mixing properties and the structure of silicate melts. *Reviews in Mineralogy and Geochemistry*, *32*(1), 147–189.

Hess, P. C. (2006). Petrogenesis of lunar troctolites—Implications for the Moon and its evolution. Proceeding of 31st Lunar and Planetary Science Conference, Abstract 1389.

Hess, P. C., & Parmentier, E. M. (1995). A model for the thermal and chemical evolution of the Moon's interior: Implications for the onset of mare volcanism. *Earth and Planetary Science Letters*, *143*, 501–514. https://doi.org/10.1016/0012-821X(95)00138-3

Hui, H., & Zhang, Y. (2007). Toward a general viscosity equation for natural anhydrous and hydrous silicate melts. *Geochimica et Cosmochimica Acta*, *71*(2), 403–416. https://doi.org/10.1016/j.gca.2006.09.003

Jolliff, B. L., & Haskin, L. A. (1995). Cogenetic rock fragments from a lunar soil: Evidence of a ferroan noritic-anorthosite pluton on the Moon. *Geochimica et Cosmochimica Acta*, *59*, 2345–2374.

Kono, Y., Irifune, T., Higo, Y., Inoue, T., & Barnhoorn, A. (2010). P-V-T relation of MgO derived by simultaneous elastic wave velocity and in situ X-ray measurements: A new pressure scale for the mantle transition region. *Physics of the Earth and Planetary Interiors*, *183*(1-2), 196–211. https://doi.org/10.1016/j.pepi.2010.03.010

Kono, Y., Kenney-Benson, C., Hummer, D., Ohfuji, H., Park, C., Shen, G., … Manning, C. E. (2014). Ultralow viscosity of carbonate melts at high pressures. *Nature Communications*, *5*, 5091. https://doi.org/10.1038/ncomms6091

Kono, Y., Kenney-Benson, C., Park, C., Shen, G., & Wang, Y. (2013). Anomaly in the viscosity of liquid KCl at high pressures. *Physical Review B*, *87*(2). https://doi.org/10.1103/PhysRevB.87.024302

Kono, Y., Kenney-Benson, C., Shibazaki, Y., Park, C., Wang, Y., & Shen, G. (2015). X-ray imaging for studying behavior of liquids at high pressures and high temperatures using Paris-Edinburgh press. *Review of Scientific Instruments*, *86*(7), 072207. https://doi.org/10.1063/1.4927227

Kono, Y., Park, C., Kenney-Benson, C., Shen, G., & Wang, Y. (2014). Toward comprehensive studies of liquids at high pressures and high temperatures: Combined structure, elastic wave velocity, and viscosity measurements in the Paris-Edinburgh cell. *Physics of the Earth and Planetary Interiors*, *228*, 269–280. https://doi.org/10.1016/j.pepi.2013.09.006

Koyaguchi, T., Hallworth, M. A., Huppert, H. E., & Sparks, S. J. (1990). Sedimentation of particles from a convecting fluid. *Nature*, *343*(6257), 447–450. https://doi.org/10.1038/343447a0

Lange, R. L., & Carmichael, I. S. E. (1990). Thermodynamic properties of silicate liquids with emphasis on density, thermal expansion and compressibility. *Reviews in Mineralogy and Geochemistry*, *24*, 25–64.

Lin, Y., Tronche, E. J., Steenstra, E. S., & van Westrenen, W. (2017a). Evidence for an early wet Moon from experimental crystallization of the lunar magma ocean. *Nature Geoscience*, *10*(1), 14–18. https://doi.org/10.1038/ngeo2845

Lin, Y., Tronche, E. J., Steenstra, E. S., & van Westrenen, W. (2017b). Experimental constraints on the solidification of a nominally dry lunar magma ocean. *Earth and Planetary Science Letters*, *471*, 104–116. https://doi.org/10.1016/j.epsl.2017.04.045

Longhi, J. (1991). Comparative liquidus equilibria of hypersthene normative basalts at low pressure. *American Mineralogist*, *76*, 785–800.

Longhi, J. (2003). A new view of lunar ferroan anorthosites: Postmagma ocean petrogenesis. *Journal of Geophysical Research 108*, 5083. https://doi.org/10.1029/2002JE001941

Longhi, J., & Ashwal, L. D. (1985). Two-stage models for lunar and terrestrial anorthosites: Petrogenesis without a magma ocean. *Journal of Geophysical Research*, *90*(S02), C571–C584. https://doi.org/10.1029/JB090iS02p0C571

Mandeville, C. W., Webster, J. D., Rutherford, M. J., Taylor, B. E., Timbal, A., & Faure, K. (2002). Determination of molar absorptivities for infrared absorption bands of H_2O in andesitic glasses. *American Mineralogist*, *87*(7), 813–821. https://doi.org/10.2138/am-2002-0702

McKenzie, D. (1984). The generation and compaction of partially molten rock. *Journal of Petroleum*, *25*(3), 713–765. https://doi.org/10.1093/petrology/25.3.713

Morse, S. A. (1982). Adcumulus growth of anorthosite at the base of the lunar crust. *Journal of Geophysical Research*, *87*(S01), A10–A18. https://doi.org/10.1029/JB087iS01p00A10

Ohtake, M., Matsunaga, T., Haruyama, J., Yokota, Y., Morota, T., Honda, C., … Josset, J. L. (2009). The global distribution of pure anorthosite on the Moon. *Nature*, *461*(7261), 236–240. https://doi.org/10.1038/nature08317

Papike, J. J., Ryder, G., & Shearer, C. K. (1998). Lunar samples. In J. J. Papike (Ed.), *Reviews in Mineralogy and Geochemistry* (Vol. 36, pp. 5.1–5.234). Washington, DC: Mineralogical Society of America.

Parmentier, E. G., Elkins-Tanton, L. T., & Schoepfer, S. (2007). Melt-solid segregation, fractional magma ocean solidification, and implications for long term planetary evolution. Proceeding of 38th Lunar and Planetary Science Conference, Abstract 1655.

Perera, V., Jackson, A. P., Gabriel, T. S. J., Elkins-Tanton, L. T., & Asphaug, E. (2017). Expedited cooling of the lunar magma ocean due to impacts. Proceeding of 48th Lunar and Planetary Science Conference, Abstract 2524.

Piskorz, D., & Stevenson, D. J. (2014). The formation of pure anorthosite on the Moon. *Icarus*, *239*, 238–243. https://doi.org/10.1016/j.icarus.2014.06.015

Ringwood, A. E., & Kesson, S. E. (1976). A dynamic model for mare basalt petrogenesis. Proceeding of 7th Lunar and Planetary Science Conference (pp. 1697-1722).

Sehlke, A., & Whittington, A. G. (2016). The viscosity of planetary tholeiitic melts: A configurational entropy model. *Geochimica et Cosmochimica Acta*, *191*, 277–299. https://doi.org/10.1016/j.gca.2016.07.027

Snyder, G. A., Taylor, L. A., & Neal, C. R. (1992). A chemical model for generating the sources of mare basalts: Combined equilibrium and fractional crystallization of the lunar magmasphere. *Geochimica et Cosmochimica Acta*, *56*, 3809–3823. https://doi.org/10.1016/0016-7037(92)90172-F

Solomatov, V. (2007). Magma oceans and primordial mantle differentiation. *Treatise on Geophysics*, *9*, 92–113.

Solomatov, V. S., Olson, P., & Stevenson, D. J. (1993). Entrainment from a bed of particles by thermal convection. *Earth and Planetary Science Letters*, *120*(3-4), 387–393. https://doi.org/10.1016/0012-821X%20(93)90252-5

Suckale, J., Elkins-Tanton, L. T., & Sethian, J. A. (2012). Crystals stirred up: 2. Numerical insights into the formation of the earliest crust on the Moon. *Journal of Geophysical Research*, *117*, E08005. https://doi.org/10.1029/2012JE004067

Taylor, S. R. (1982). *Planetary science: A lunar perspective*. Houston TX: Lunar and Planetary Institute.

Vander Kaaden, K. E., Agee, C. B., & McCubbin, F. M. (2015). Density and compressibility of the molten lunar picritic glasses: Implications for the roles of Ti and Fe in the structures of silicate melts. *Geochimica et Cosmochimica Acta*, *149*, 1–20. https://doi.org/10.1016/j.gca.2014.10.029

Vetere, F., Behrens, H., Holtz, F., & Neuville, D. R. (2006). Viscosity of andesitic melts—New experimental data and a revised calculation model. *Chemical Geology*, *228*(4), 233–245. https://doi.org/10.1016/j.chemgeo.2005.10.009

Walker, D. (1983). Lunar and terrestrial crust formation. *Journal of Geophysical Research*, *88*(S01), B17–B25. https://doi.org/10.1029/JB088iS01p00B17

Walker, D., & Hays, J. F. (1977). Plagioclase flotation and lunar crust formation. *Geology*, *5*(7), 425–428. https://doi.org/10.1130/0091-7613(1977)5%3C425:PFALCF%3E2.0.CO;2

Walker, D., Longhi, J., & Hays, J. F. (1975). Differentiation of a very thick magma body and implications for the source region of mare basalts. Proceeding of 6th Lunar and Planetary Science Conference (pp. 1103-1120).

Walker, D., Powell,M. A., Lofgren, G. E., & Hays, J. F. (1978). Dynamic crystallization of a eucrite basalt. Proceeding of 9th Lunar and Planetary Science Conference (pp. 1369-1391).

Warren, P. H. (1990). Lunar anorthosites and the magma-ocean plagioclase-flotation hypothesis: Importance of FeO enrichment in the parent magma. *American Mineralogist*, *75*, 46–58.

Wood, J. A., Dickey, J. S., Marvin, U. B., & Powell, B. N. (1970). Lunar anorthosites and a geophysical model of the Moon. Proceeding of 11th Lunar and Planetary Science Conference (Vol. 1, pp. 965–988).